# BUILDINGS OBSTRUCTION EFFECT ON POWER PERFORMANCE OF SMALL WIND TURBINE USING 3 TURBULENCE MODELS CFD TECHNIQUE

**[1]KRITTAPAS KONGKAPISUTH, [2]WIRACHAI ROYNARIN, [3]DECHA INTHOLO**

Engineering Faculty, Rajamangala University of Technology Thanyaburi (RMUTT), PhathumthaniThailand 12110
E-mail - [1]krittapas_k@mail.rmutt.ac.th, [2]wirachai_r@rmutt.ac.th, [3]decha_i@rmutt.ac.th

**Abstract -** Horizontal Axis Wind Turbines (HAWTs) are commonly used in the wind energy sector. Small HAWTs are the most efficient wind machines that can harness wind energy to support on-grid and of-grid applications. The wind technologies are installed in urban areas near buildings or vegetation and these are known to obstruct wind flow. The basic challenges of wind turbines (WTs) installed in urban areas are low energy yield and unpredictability of stall due to the effects of turbulence wind flow arising from obstructions. This study focus on phenomenon associated with wind flow influence on three SWTs, 5kW HAWTs (WT1, WT2, and WT3), located at the Defense Energy Training Center (DTEC). The objective of the study is to investigate the wind turbines power performance effect as wind flow across building obstruction in DETC from South-West (SW) direction, one of main direction of wind flow in Thailand, using Computational Fluid Dynamics (CFD) k-ε, k-ω, and RNG turbulence model with allowing rotating region, rotational wind turbines, into CFD condition. From the results of CFD simulations compare to WT0, wind turbine without obstruction, it is observed that; using k-ε model, WT1-WT2 increased by 7.73 %, and 5.68 % respectively while WT3 decreased by 7.50 %. Using k-ω model, WT1-WT2 increased by 9.84 %, and 14.54 % respectively while WT3 decreased by 2.23 %. Using RNG model,WT1-WT2 increased by 6.41 %, and 10.60 % respectively while WT3 decreased by 5.19 %. For the results of power performance effect, wind turbines in buildings obstruction wind flow area does not always created low energy yield due to the fact that they may cause Venturi effect, steeply wind shear gradient, etc. that can create increased or decreased power performance. And also from the CFD, the three turbulence models displayed show similar results that affirmed that this technique is highly reliable. However, the most significant procedure of this CFD technique is allowing rotating region, rotational wind turbines, into CFD condition.

**Index Terms -** Computational Fluid Dynamics (CFD), Horizontal Axis Wind Turbines (HAWTs), Building obstruction wind flow area, CFD k-ε, k-ω, and RNG turbulence model.

## INTRODUCTION

### A. Wind Energy

Renewable energy resources such as solar, wind, hydro, tides, waves, geothermal, biomass, and etc. are replenished by nature and as a result of human activities on earth. Generally, these Alternative Energy Sources can provide the energy needs in areas such as electricity production, thermal, fuel, and off-grid energy services. Based on REN21's 2016 report, Renewable energy utilization is about 8.9% of the world energy need, and 2.2% of this supply from renewable energy is channeled to electricity production and they are generated from wind, solar, geothermal, and biomass [1]. Currently, world energy consumption is unceasingly increasing, nevertheless, renewable energy has the potential to supply abundant of clean energy if the resources can be efficiently harnessed [2]. Wind energy has been identified as a reliable source of renewable energy. A wind turbine is a device that converts wind's kinetic energy into electrical power. Wind turbines are usually installed base on an accurate or approximated study of wind resource but the design is always constrained by socio-economic and environmental concerns. Mostly, suitable site for wind turbines with good performance is in the windy areas and far from obstacles to wind flow directions. Small wind turbines, HAWTs, can be used to fulfill the energy needs of the urban society. Their production can also be harnessed to support the on-grid and off-grid applications [3][4][5][6]. Turbulence flow is a common phenomenon in wind energy and is often characterized by unsteady performance of wind turbine [7]. Therefore it is necessary to investigate the effects of turbulence intensity and vortex on wind turbine for improvement of power performance of any intended installation [8]. The challenges of small wind turbine in such area is getting low energy yield from low mean wind speed due to Eddies and swirls. 'Turbulence' also hinders good performance for wind turbines because wind profile in such area is different from open area [9][10]. Turbulence is caused not only by obstacles, but also by the topography of the landscape. Turbulence and laminar flow are shown in Figure 1.

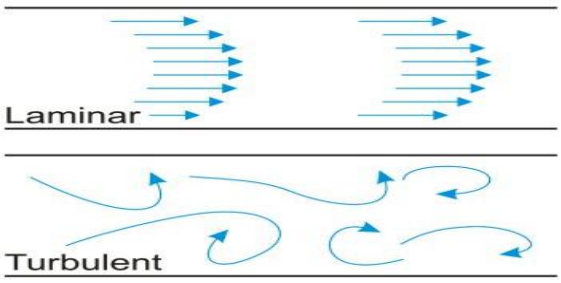



**Figure 1.Turbulent and Laminar Flow [10]**

The wind speed distribution depends on the type of air flow in the atmospheric boundary layer and varies as a function of the altitude and the site topography. Figure

2 Shows wind flow deflected from its path when it encounters an obstacle. Wind flows around the obstacle, speeding up as it passes around the sides and over the top of the obstacle, while creating a slower and more turbulent wind area that continues for a distance behind the obstacle [11].

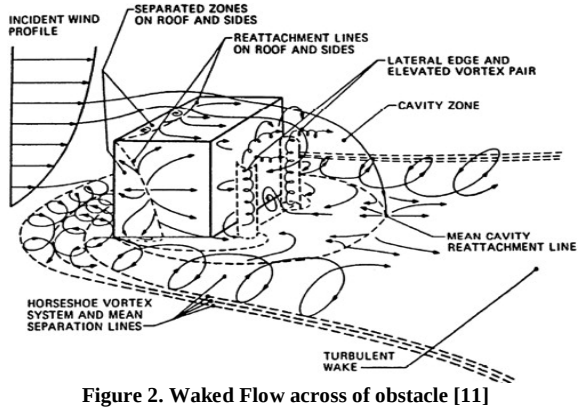



**Figure 2. Waked Flow across of obstacle [11]**

Wind turbines are designed to performance in the most efficient ways but building obstruction airflow can cause wind flow impedances leading to inefficiency and irregularity. The behavior of a WT in the field is affected by wind speed and wind flow direction. At each change of direction and speed, the turbine will try to adapt to the new conditions and the transition usually influence energy production negatively. In other words, the reason behind the limited installation of small wind turbines in buildings obstruction wind flow areas are the low mean wind speeds and the high level of turbulence encountered in those scenarios [12]. Therefore, before installation of wind turbines in such areas, proper analysis and prediction of performance is necessarily. This can be estimated by using CFD technique that are simple, accurate, and reduce cost and time.

### B. Turbine Performance

Expected turbine performance is demonstrated by the manufacturer's power curve. The manufacturer's power curve is typically derived from test data in ideal wind conditions. Data from non-ideal wind conditions are filtered out of the analysis so that results demonstrate the turbine's performance when subjected to un-waked horizontal non-turbulent flow at sea-level air density. Although some installation site parameters may be close to ideal conditions, others, particularly those in urban environments, will exhibit less ideal conditions. This is established by lower power production at these locations, indicated by a drop in the manufacturer's power curve. Figure 3 presents an example of power curve and demonstrates how energy production may be lower in non-ideal wind conditions. Therefore, expected energy production at turbine locations requires adjustment to reflect performance based on the real conditions experienced at the site. For a steady turbulent shear flow, the mean velocity profile in a small region near the surface is described by the relationship called the Wall law:

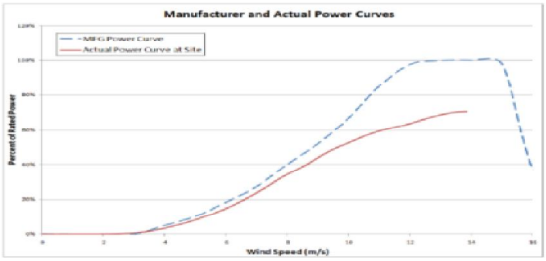



**Figure 3. Power curve between manufacturer and site installation**

$$\frac{u_t}{u^*} = \frac{1}{2}\ln\left(\frac{z}{z_0}\right) + B \qquad (1)$$

where $u^*$ is the friction velocity, K is the von Karman constant (K = 0.42 ), B is an empirical constant related to the thickness of the viscous sublayer ( B = 5.2 in a boundary layer over a smooth flat plane; for rough walls, smaller values of B are obtained) [13]. The constant $z_0$ called roughness is the frontier between the logarithmic zone and the inner $k-\varepsilon$ zone. When wind speed changes direction with increasing height above ground, it is known as the shear gradient. The wind shear formula is shown below:

$$U = U_{ref}\left(\frac{h}{h_{ref}}\right)^{\alpha} \qquad (2)$$

where U and U_ref represent the wind speed at height h, and h_ref represent the height of interest and the reference height respectively, $\alpha$ represents the site/condition specific shear exponent. In relation with a mild shear gradient ($\alpha \leq 0.1$), wind conditions are generally uniform across a turbine's rotor plane, provided a conditions with a sharp shear gradient ($\alpha \geq 0.3$) is maintained.

### C. Computational fluid dynamics

Computational fluid dynamics (CFD) is a simulation of fluid mechanics for solving and analyzing fluid flows. It can be applied to predict accurate wind turbine performance together with minimum or optimum cost and time scale. And the CFD result can be compared to experimental method. In computational modeling of turbulent flows, the appropriate model that comply with the type of obstruction can predict fluid velocity and most of relevant issues for engineering design which involve fluid flows [10]. A CFD turbulence model has a procedure to close the system of mean flow equations, it is not necessary for engineers to resolve the detail of turbulent fluctuations. It is only needed to know how turbulence affects the mean flow. Useful turbulence models must have wide applicability that are accurate, simple, and economical to run. Most classical models based on Reynolds Averaged Navier-Stokes (RANS) equations (time averaged) e.g. Zero equation model: mixing length model, one equation model, two equation models: k-ε style models (standard, RNG, realizable), k-ω model etc. [14]. The

Reynolds-averaged approach is based on decomposing the velocity as

$u_j = \bar{u}_j + \acute{u}_j$(3)

where $\bar{u}_j$ is the average velocity vector and $\acute{u}_j$ is the velocity vector fluctuation. The $k-\varepsilon$ model was found to give more effective response to the energy production rate than does the standard $k-\varepsilon$ turbulence model. The $k-\varepsilon$ model equations is written below:

$$\rho(\bar{U}.\nabla)K = \nabla\left[\left(\mu + \frac{\mu_t}{\sigma_k}\right)\nabla K\right] + P_k - \rho \quad (4)$$

$$\rho(\bar{U}.\nabla)\varepsilon = \nabla\left[\left(\mu + \frac{\mu_t}{\sigma_\varepsilon}\right)\nabla\varepsilon\right] + C_{\varepsilon 1}\frac{\varepsilon}{K}P_k - C_{\varepsilon 1}\rho\frac{\varepsilon^2}{K} \quad (5)$$

$$\mu_t = \rho C_\mu \frac{K^2}{\varepsilon} \quad (6)$$

$$P_k = \mu_t[\nabla\bar{U} + (\nabla\bar{U})^t]\nabla\bar{U} \quad (7)$$

The adaptation of the standard model constants which is applicable to flows with high Reynolds numbers is given in table 1. The reasons of selecting CFD k-ε, k-ω, and RNG turbulence models to validate the performance prediction of the turbine is because the characteristic of CFD k-ε, k-ω, and RNG turbulence models are most appropriate for the given conditions of the study [15][16][17]

**D. $k-\varepsilon$ Turbulence Model;**

- The CFD $k-\varepsilon$ turbulence model most widely used and validated with applications ranging from industrial to environmental flows.
- The model is useful for free-shear layer flows with relatively small pressure gradients in confined flows where the Reynolds shear stresses are important.
- The model can be stated as the simplest model for which only initial and/or boundary conditions needs to be supplied.
- There are two- equations for Von-Karman Constant (k) and, together with the eddy-viscosity stress strain relationship constitute the k-ε model, and many attempts to develop two-equation models that improve on the $k-\varepsilon$ model: where ε is the dissipation rate of k.

**E. $k-\omega$ Turbulence Model;**

- One of the most commonly used turbulence models. It is a two equation model, includes two extra transport equations to represent the turbulent properties of the flow.
- It is the variable that determines the scale of the turbulence, whereas the first variable, Ɛ, determines the energy in the turbulence.
- This allows a two equation model to account for history effects like convection and diffusion of turbulent energy.

**F. Rng Turbulence Model;**

- The model was developed using Re-Normalisation Group (RNG) methods to normalize the Navier-Stokes Equations, to account for the effects of smaller scales of motion.
- It can be used to derive a turbulence model similar to the k-Ɛ model, results in a modified form of the epsilon equation which attempts to account for the different scales of motion through changes to the production term.
- The RNG model in FLUENT provides an option to account for the effects of swirl or rotation by modifying the turbulent viscosity appropriately.
- Similar k- ε equations includes additional term in • equation for interaction between turbulence dissipation and mean shear, the effect of swirl on turbulence, analytical formula for turbulent Prandtl number, and differential formula for effective viscosity.

However, CFD simulations are sensitive to the large range of computational parameters that have to be set by the user. Hence, before doing any wind study project, a comparison of computational results with measured data must be performed for the different discretization schemes. Additionally each scheme has to be tested against the multiple turbulence models with respect to the grid dependency tests [18]. Computational Fluid Dynamics is a branch of Fluid Mechanics where numerical methods are used to solve the governing equations describing the behavior of fluid flow. The governing equations are based on three fundamental principles of conservation. The continuity equation (or conservation of mass), the momentum equation, obtained by applying Newton's law of motion to a fluid element, and the energy equation (conservation of energy) based on the 1st law of thermodynamics. The governing equations, including the Navier-Stokes equation, developed by M. Navier and G. Stokes in the first half of the 19th century, are presented in their most general form as below.

Continuity equation

$$\frac{\partial\rho}{\partial t} + \nabla\cdot(\rho\vec{u}) = 0 \quad (8)$$

Momentum Equation

$$\Sigma F = ma \quad (9)$$

Expressed as the Navier-Stokes Equation:

$$\frac{\partial}{\partial t}(\rho\vec{u}) + \rho(\vec{u}\cdot\nabla\vec{u}) = -\nabla p + \nabla\cdot\tau + S_m \quad (10)$$

Where the stress tensor $\tau$ is related to the strain rate by

$$\tau = \mu\left(\nabla\vec{u} + (\nabla\vec{u})^T - \frac{2}{3}\delta\nabla\vec{u}\right) \quad (11)$$

Energy equation

$$\frac{\partial}{\partial t}(\rho h_t) - \frac{\partial\rho}{\partial t} + \nabla\cdot(\rho\vec{u}h_t) = \nabla\cdot(\vec{u}\cdot\tau) + \vec{u}\cdot S_m + S_e \quad (12)$$

Where the total enthalpy $h_t$ is related to the static enthalpy, $h_s$ by:

$$h_t = h_s + \frac{1}{2}\vec{u} \quad (13)$$

There is no analytical model to governing equations for the complex flow geometries and discretization of numerical of series expansions. The partial differentials are carried out in order to approximate the solutions solving. This numerical technique is the underlying principle of CFD. The assumptions are

usually allowed to simplify the equations. Removing some parameters in some cases will help to correct the whole equation to solve the problem. It is assumed that the fluid flow is steady, isothermal, and incompressible.

CFD methods are constantly being developed to improve computational resource capability, CFD has reached the stage where analysis of complex phenomena such as multiphase, free surface, highly turbulent flows is possible for a large number of design variations in a reasonable timescale [19]. Recently, developments of CFD codes have shown that the simulation of this nature is in good agreement with experimental data [20]. Giving the confidence to the reliable of the numerical results.

The CFD program used to carry out the simulations of a finite-volume method is also used for the spatial discretization of the governing equations. The numerical method should be validated. The study should compare to the experimental method [21] and the flow feature in small wind turbine will be investigated.

**Venturi Effect**

Venturi effect is named after Giovanni Battista Venturi (1746–1822), an Italian physicist. The Venturi effect is the reduction in fluid pressure that results when a fluid flows through a constricted section. Analysis shows that in a situation with constant mechanical energy, the velocity of a fluid passing through a constricted area will increase and its static pressure will decrease. This phenomenon utilizes both the principle of continuity equation as well as the principle of conservation of mechanical energy and can be observed in both nature and industry. Venturi effect increases wind speed when it funnels through small openings. The severityof Venturi effect is a function of width, length, height, and size of openings in the canyon. Venturi effect is seen when winds funnel through small openings, further enhancing the acceleration of winds [22] and both these effects are explained by the Bernoulli's principle.

**G. Objective of the Study**

The objective of this paper is to investigate the power performance effect of three 5 kW HAWTs as wind flow across buildings obstruction from South-West (SW), one of the main direction wind flow in Thailand, by using CFD k-ε, k-ω, and RNG turbulence model with allowing rotating region, rotational wind turbines, into CFD condition. In the scenario of CFD turbulence models simulation, three 5 kW HAWTs with hub height 18 m and blade diameter 6.4 m be installed among four main concrete buildings of buildings' height 9.25, 13.30, and 15.0 with incoming wind speed 4.5 m/s.

## II. EXPERIMENTAL DETAILS

A. **Model Description**

The site of study, Defence Energy Training Center (DETC), is considered as building obstruction wind flow area. In this case, there are three 5kW HAWTs, THUNYA-5 kW HAWT, with four main buildings constructed as shown in Figure 4. DETC is located at Rayong province, Thailand. The site position is on latitude 12 degrees 40 minutes North, longitude 101 degrees 2 minutes East, and height of 3 m above sea level. Wind blows throughout the year including in the South-West monsoon season from May to October, and the North-East monsoon from November to January. The statistical data of wind speed in the past 30 years of Rayong province (between 1968 to 1997) from the Data Processing Division of the Department of Meteorology shows that the average of wind speed is between 2.6 to 7.7 m/s. The highest wind speed occurs between June to August. [23] Figure 4 and Table 2 describes the model, sizing, and alignment of buildings and the wind turbines in DETC.

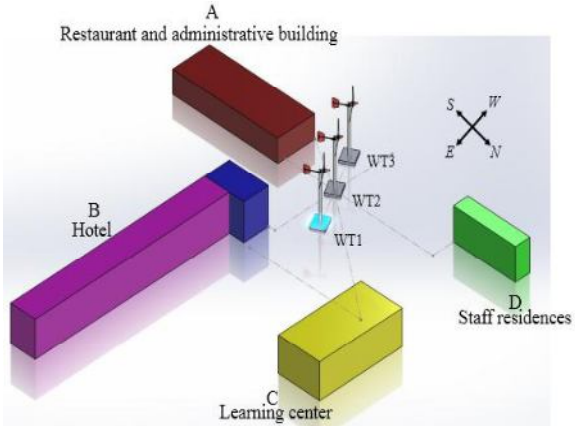



**Figure 4. Buildings Model of DETC**

| Building | Height (m) | Width (m) | Length (m) | Distance From WT1 | Distance From WT2 | Distance From WT3 |
|---|---|---|---|---|---|---|
| A | 9.25 | 18 | 51 | 35 | 24 | 20 |
| B | 15 | 12 | 113 | 25 | 30 | 45 |
| C | 9.25 | 18 | 51 | 60 | 70 | 87.5 |
| D | 13.30 | 7 | 30 | 47.5 | 50 | 55 |

**Table 2 Sizing and alignment of buildings and wind Turbines in DTEC.**

**Remarks;** the wind turbines have a distance of 18 m between each other, a three dimensional model of the buildings and wind resource data was used as input to the CFD model and completed by CFDesign commercial program. Energy production data was

obtained for the turbines and compared to the results from the CFD analysis as well as the theoretical energy production. In this study, WT1, WT2, WT3 are the represents the case study 5 kW HAWTs whose performance effect are investigated as wind flow across building obstruction using CFD k-ε, k-ω, and RNG turbulence model with CFDesign V.7 software. The results of this study is expected to show the percentage of effectiveness of wind turbines power performance compared to wind turbines power performance of a 5 kW HAWT, WT0, arbitrary located in the site without buildings obstruction at the turbine blade of diameter 6.4 m after incoming wind speed at 4.5 m/s flows pass through influence buildings.

B. **CFD Boundary Conditions**

When solving CFD problems, the Navier-Stokes equation and continuity equations, appropriate initial conditions and boundary conditions need to be applied. Figure 5 shows the CFD boundary conditions of the model, 3D model, is applied by control volume for simulation. The model included two main condition. First is fixed condition obtained by the buildings and the ground. Second is moving condition obtained by the wind turbine blades and air. Inlet condition of 4.5m/s wind velocity is selected and outlet condition is selected at 0 Pa of wind gage pressure.

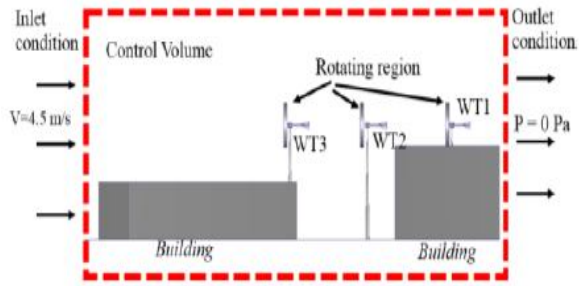



**Figure 5. CFD Boundary conditions**

| Parameter name | Unit | Parameter Value |
|---|---|---|
| Inlet velocity | m/s | 4.5 |
| Inlet Total Temperature | K | 320 |
| Angular Velocity | rpm | Free spin |
| Working fluid | | Ideal Air |
| Fluid Density | $kg/m^3$ | 1.225 |
| Turbulence Model | | $k-\varepsilon$ |
| Outlet | Pa | 0 |

**Table 3 CFD Model Parameters**

This model produces a steady state solution with some account of the interaction between the two frames. The quasi-steady approximation involved becomes small when the passing flow speed is large relative to the turbine speed at the interface. The boundary conditions control volume parameters is shown in Table 3.

Table 3 shows the model parameters which are applied in CFD control volume model with inlet side selected by wind velocity while outlet side is selected by pressure. Ideal air was used for working fluid and the k-ε, k-ω, and RNG turbulence model was applied for simulation.

CFD modeling is conducted to assess wind flows and estimate system of energy output, accounting to the specific geometries of obstacles flows. The site geometry was modeled using Computer Aided Design (CAD). Wind conditions were expected on the geometry model to estimate the flow conditions resulting from the interaction between wind flow, building structures, ground roughness, and wind turbines. A detailed explanation is presented below.

CFD modeling is conducted to assess wind flows and estimate system of energy output, accounting to the specific geometries of obstacles flows. The site geometry was modeled using Computer Aided Design (CAD). Wind conditions were expected on the geometry model to estimate the flow conditions resulting from the interaction between wind flow, building structures, ground roughness, and wind turbines. A detailed explanation is presented below.

C. **Model Description of Mesh Refinement Study**

Figure 6 shows the CFD tetrahedron mesh model along with the buildings in DTEC. The CFD model generated 1.5 million elements for buildings, 1.2 million elements for wind turbine, 2.3 million elements for air, and 0.7 million elements for ground.

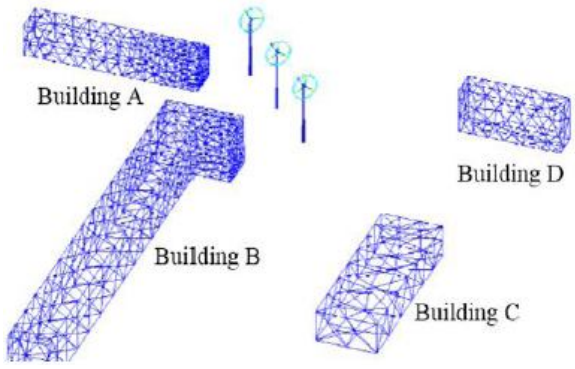



**Figure 6. Meshing of DTEC Buildings Model**

The CFD mesh adaptation system was used to refine the mesh in specified where the velocity gradients were high of volume for investigation. Three mesh adaptation steps also were undertaken of each model called “Coarse Mesh”, “Medium Mesh”, “Fine Mesh”.

## III. RESULTS AND DISCUSSION

Figure 7(a1)-(d3) shows wind flow profile of CFD k-ε, k-ω, and RNG turbulence model with allowing rotating region, rotational wind turbines, into CFD condition results from SW direction at the different height, 9.25, 13.30, 15.0, and 18.0 m, of cutting plane from the ground. The points of cutting plane determined by the inflow of wind velocity, turbulence intensity, recirculation zones, and represents the location on the buildings' roof. The wind velocity profile indicated that: At higher points of cutting plane there are more wind velocity, and predominantly brings about Venturi effect by building A-B.

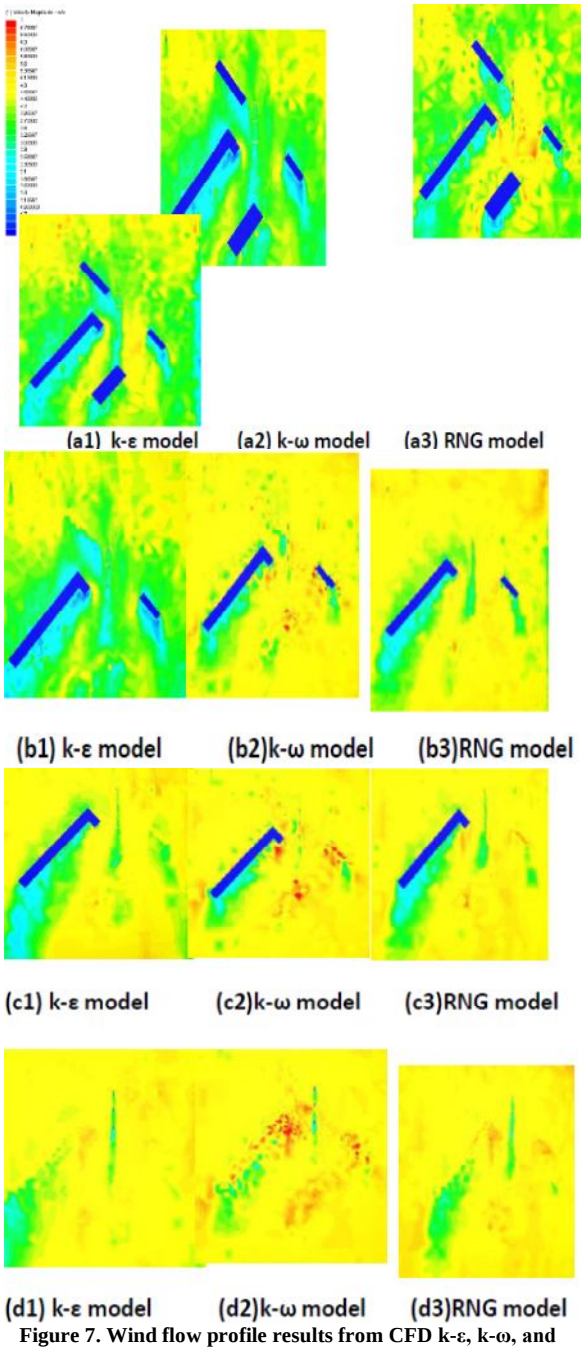



**Figure 7. Wind flow profile results from CFD k-ε, k-ω, and RNG turbulence model simulation, at height (a) 9.25 m (b) 13.30 m (c) 15.0 m (d) 18.0 m**

Moreover, at the height 18.0 m, wind turbine hub-height, steeply wind shear gradient are obtainable from the building influences causing increasing or decreasing wind speed to the turbines.

Figure 8(a), (b), and (c) shows the similarly wind velocity contour of WT3, WT2, and WT1 from CFD k-Ɛ, k-ω, and RNG turbulence model results. The results show that even though the DETC area has more open terrain nearby WT3 but the wind velocity contour of WT3 likely less than wind velocity of WT2 and WT1.

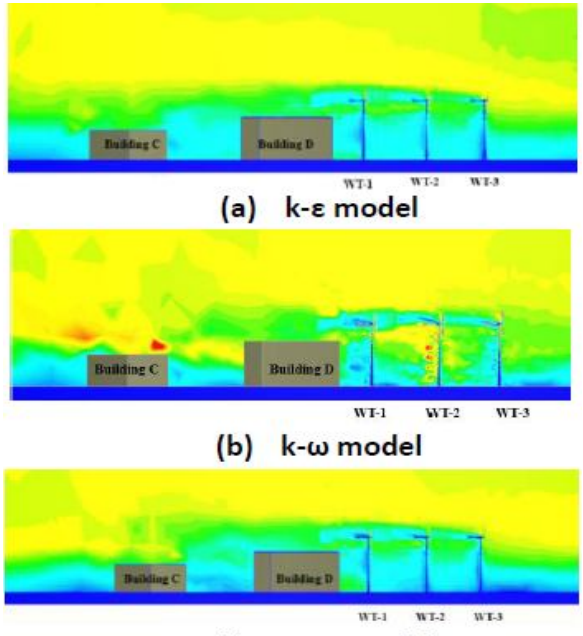



**Figure 8Wind velocity contour of WT1-WT3 simulated by CFD**

Figure 9 shows the example of air accelerating over buildings and created steep shear gradients with non-uniform shear gradients as shown. Owning that the local wind shear gradients can be generated above a roof surface as wind flow passing over the building and leave low wind speed region immediately above the roof and then make transitions steeply to higher wind speed zone. Therefore, wind flow from SW increase wind speed to WT2-WT1 notonly create by Venturi effect between building A-B but also by the steeply wind shear gradient from building A and B while wind flow from SW decrease wind speed to WT3 due to vortex nearby building A influence to WT3.

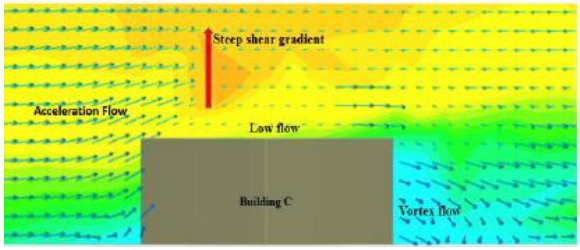
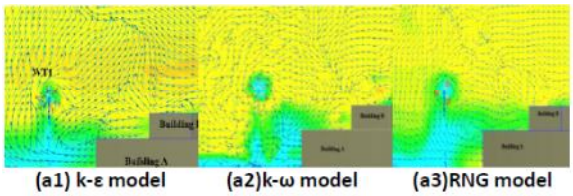
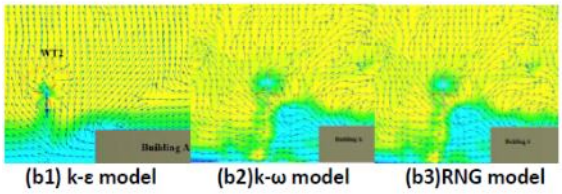
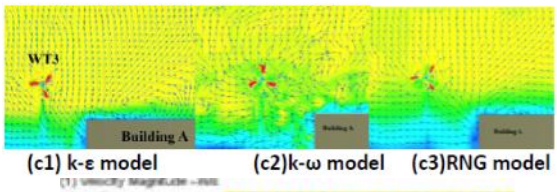


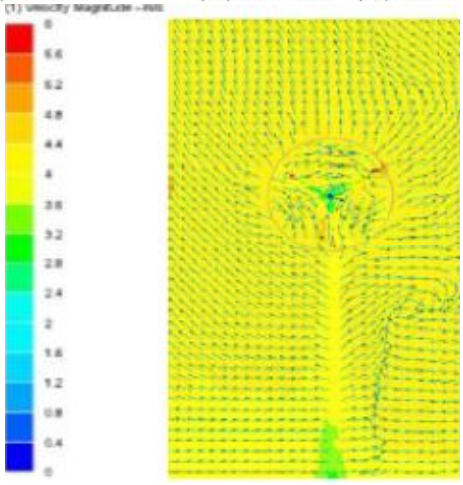

**Figure 9 Air accelerating over buildings and created Steep Shear Gradient**

Figure 10(a1-c3), and (d) shows the vector of vortex flow at wind turbines from SW direction generated vortex beside WT1-WT3 from each CFD turbulence model. WT1-WT3 are installed behind the buildings and behind the front turbines, therefore, vortex flow is depicted in WT1-WT3 but no vortex flow is depicted on WT0 since it is an arbitrary installation in area without building obstruction.



**(d) No vortex flow at WT0,**
**Figure 10(a1)-(c3) Vector of Vortex flow to WT1-WT3, using CFD k-Ɛ, k-ω, and RNG turbulence model**

## RESULTS

Figure 11 and Table 4 above shows the power performance effect results of wind turbines, WT1-WT3, using CFD k-Ɛ, k-ω, and RNG turbulence model simulation technique that they are increase and decrease by compare to a wind turbine without obstruction, WT0, as wind flow from SW in DETC. It is showed that; Using k-ε model, the power performance of WT1-WT2 increased by 7.73 %, and 5.68 % respectively while the power performance of WT3 decreased by 7.50 %. Using k-ω model, the power performance of WT1-WT2 increased by 9.84 %, and 14.54 % respectively while the power performance of WT3 decreased by 2.23 %. Using RNG model, the power performance of WT1-WT2 increased by 6.41 %, and 10.60 % respectively while the power performance of WT3 decreased by 5.19 %.

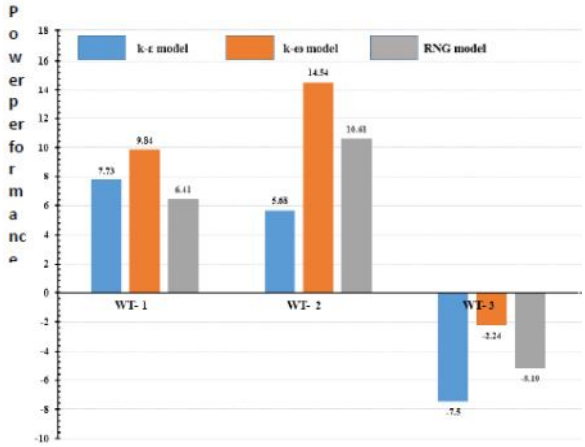



**Figure 11 the power performance effect results of wind turbines**

| Wind Turbine No. | Wind Turbine Power(k-ε )(%) | Wind Turbine Power(k-ω) (%) | Wind Turbine Power RNG(%) |
|---|---|---|---|
| WT0 | 100.00 | 100.00 | 100.00 |
| WT1 | +7.73 | +9.84 | +6.48 |
| WT2 | +5.68 | +14.54 | +10.62 |
| WT3 | -7.5 | -2.24 | -5.89 |

**Table 4 The results of wind turbines power performance effect using CFD k-Ɛ, k-ω, and RNG turbulence model**

## DISCUSSIONS

For the results of power performance effect; Normally, the geometric features of buildings and front turbines obstruction structures cause the layouts to have major effects in wind flow characteristic, speed, direction, and frequency, towards wind turbines power performance due to buildings obstructions as wells as front turbines turbulence phenomena. These resulted in unexpected change in direction, speed, and frequency of the wind. And also geometric features of buildings slows down wind speed: they can also channel wind flow into canyon among space area of buildings and lead to increase in wind speed as a result of the overpressure of wind flow between buildings with the Venturi effect that can increase the frequency of turbulent winds. Meanwhile, front turbines and geometric features of buildings can create vortex and steep shear gradient leading to wind flow characteristic, speed, direction, and frequency, that have increase or decrease of wind turbines performance. Moreover, if the temperature increased within canyon among space area of buildings obstruction, it can create low pressure cell and lead to frequency and increase wind speed also. In addition to, widely spaced buildings can act as single isolated blocks, therefore, if the gap decreases between buildings, the wind flow will likely becomes more and more subject to overpressure and thus the Venturi

effect can change the frequencies of airflow by producing a complex pattern of changes in wind direction and speed. From the results, incoming wind flow from SW creates Venturi effect by channel incoming wind flow into canyon among space area of buildings by building A-B, and also building A creates steeply wind shear gradient that lead to increase power performance of WT1 and WT2 while power performance of WT3 is decreased since WT3 is not in canyon space area of buildings, and also building A creates more vortex flow effect to WT3. As the results from CFD k-Ɛ, k-ω, and RNG turbulence model simulations;The results of CFD k-Ɛ, k-ω, and RNG turbulence model profile appearance are similar effectible of wind turbines, WT1, WT2, and WT3, power performance that affirmed this technique is highly reliable. In summary of discussion are as follows;

- Power performance at WT3 decrease likely by wake region from Building A due to the position of WT3 close to Building A.
- Power performance at WT2 increased likely by Venturi effect that created from Building A-B, and by steep shear gradient from Building A.
- Power performance atWT1 increased likely by Venturi effect that created from Building A-B, and by steep shear gradient from Building A and Building B.
- The results of CFD k-Ɛ, k-ω, and RNG turbulence model profile appearance are similar effectible of wind turbines that affirmed this technique is highly reliable.

Hence, not only in buildings obstruction wind flow area does not always create wind power into low energy yield due to they may cause Venturi effect and steeply wind shear gradient, and etc. that can create increased and decrease wind turbines power performance, but also, the CFD turbulence model simulation technique is reliable for using to predict the tendency of wind turbines power performance and could be applied in terms of small HAWTs installation in the buildings obstruction wind flow area.

## CONCLUSIONS

With reference to the results and discussions of the wind turbines power performance from CFD three turbulence models simulation compare to non-obstruction wind turbine, and the profile appearance of CFD three turbulence models above, the conclusions are as follows;

1. The results of this CFD investigation of wind turbines with their position in the site showed that the results can be applied to making design plans in terms of appropriate parameters required to get higher plant factor of wind turbines.
2. Wind turbine power performance in buildings obstruction wind flow area does not always create wind power with low energy yield since they may cause Venturi effect and steep wind shear gradient that can create increased or decrease wind turbines power performance.
3. Hence, when choosing buildings obstruction wind flow area to install wind turbines, some major factor that have to be considered are the geometric features of buildings obstruction layout which get along well with the wind flow pattern to the wind turbines. This is a fair evaluation because buildings obstruction can cause positive Venturi effect to channel the canyon and steep wind shear gradient for increasing wind turbines power performance.
4. Rotating region, rotational wind turbines, is the most necessary to allow in the CFD conditions due to their procedure have ability to enhance the accurate of the simulation results.
5. The results of CFD three turbulence models simulation technique is not only according to the related theory but also the numerical results effect are reliable for predicting the power performance profile of wind turbines in the site.
6. Consequently, this CFD simulation technique can be applied in decision making in plant positioning and locating of wind turbines for the best points of the site, and for estimating wind turbine plant factor in promising areas. On the other hand, this technique can also significantly save cost and time: it can be applied in making reliable capable tool of wind turbines power performance prediction, optimization of wind turbines locating point, buildings obstruction influence manner, project's cost-benefit analysis, etc..

Further works are proposed to the process of validation to the CFD three turbulence models and the power performance effect of the three 5 kW HAWTs by comparing the results of the three turbulence CFD models and power performance effect with the site estimated or site measurement results. Therefore, the result of further works will help to validate this technique, and to showcase which one of the three turbulence model could be the most suitable to apply in terms of small wind turbines installation in the buildings obstruction wind flow area.

## ACKNOWLEDGEMENTS

I would like to thanks all that assisted in this study including the team in Energy Research and Service Center (ERSC) of engineering faculty, RMUTT who supported my work and help me in getting quality and accurate analysis. I am very grateful to my supervisor, Asst. Prof. Dr.Wirachai Roynarin for his patience and support in overcoming numerous obstacles that I had face in the process of conducting my study. Additionally, I would like to thanks all friends who supported and motivated me in one way or another. I would also like to thanks my family for their spiritually encouragement throughout the writing process of this paper.

## REFERENCES


[1] R. Burrett, R. Dixon, M. Eckhart, D. Hales, and A. Kloke-lesch, "Renewables Global Status Report," p. 32, 2016.

[2] A. BashirzadehTabrizi, J. Whale, T. Lyons, and T. Urmee, "Performance and safety of rooftop wind turbines: Use of CFD to gain insight into inflow conditions," Renew. Engery, vol. 67, p. Pages 242-251.

[3] N. J. Choi, S. H. Nam, J. S. Kim, S. M. Lee, and K. C. Kim, "CFD study on power output and flow characteristics of 110 kW class BAWT," in Proceedings of the 2011 International Conference on High Performance Computing and Simulation, HPCS 2011, 2011, pp. 859–864

[4] J. K. Kaldellis and D. Zafirakis, "The wind energy (r)evolution: A short review of a long history," Renew. Energy, vol. 36, no. 7, pp. 1887–1901, 2011.

[5] A. Sengupta, A. Biswas, R. Gupta, and N. Srinagar, "Vertical Axis Wind Turbines in the Built Environment- A Review," ISESCO J. Sci. Technol., vol. 12, pp. 1–4, 2016.

[6] S. Stankovic, N. Campbell, and A. Harries, "Urban Wind Energy," Earthscan, 2009.

[7] Q. Li et al., "Study on power performance for straight-bladed vertical axis wind turbine by field and wind tunnel test," Renew. Energy, vol. 90, pp. 291–300, 2016.

[8] Q. Li, J. Murata, M. Endo, T. Maeda, and Y. Kamada, "Experimental and numerical investigation of the effect of turbulent inflow on a Horizontal Axis Wind Turbine (Part I: Power performance)," Energy, vol. 113, pp. 713–722, 2016.

[9] F. Balduzzi, A. Bianchini, E. A. Carnevale, L. Ferrari, and S. Magnani, "Feasibility analysis of a Darrieus VAWT installation in the rooftop of a building," Int. Conf. Appl. Energy, no. May, pp. 3345–3358, 2011.

[10] A. B. Tabrizi, J. Whale, T. Lyons, and T. Urmee, "Performance and safety of rooftop wind turbines: Use of CFD to gain insight into inflow conditions," Renew. Energy, vol. 67, pp. 242–251, 2014.

[11] E. Burton, T.; Sharpe, D.; Bossanyi, Wind Energy: Handbok. 2001.

[12] L. Ledo, P. B. Kosasih, and P. Cooper, "Roof mounting site analysis for micro-wind turbines," Renew. Energy, vol. 36, no. 5, pp. 1379–1391, 2011.

[13] Y. Wan, E. Ela, and K. Orwig, "Development of an Equivalent Wind Plant Power-Curve Preprint," Wind. 2010, no. June, p. 20, 2010.

[14] D. Launder, B &Spalding, "The Numerical computation of turbulent flows,computer methods in applied mechanics and Engineering," vol. 3, pp. 201–225, 1972.

[15] T. Cebeci, "Turbulence models and their applications," 10th Indo Ger. Winter Acad., 1984.

[16] Bert Blocken, "CFD Simulation pf Wind Environmental Conditions over Natural Complex Terrain," Work. Trends Challenges Wind Energy Harvest., pp. 30–31, 2015.

[17] D. Choudhury., "Introduction to the Renormalization Group Method and Turbulence Modeling" Fluent Inc., Technical Memorandum TM-107, 1993.

[18] L. A. Danao, "The Influence of Unsteady Wind on the Performance and Aerodynamics of Vertical Axis Wind Turbines," pp. 1–258, 2012.

[19] F. R. Menter, R. Langtry, and S. Völker, "Transition modelling for general purpose CFD codes," Flow, Turbul. Combust., vol. 77, no. 1–4, pp. 277–303, 2006.

[20] P. Bachant and M. Wosnik, "Effects of Reynolds Number on the Performance and Near-Wake Dynamics of a Vertical-Axis Cross-Flow Turbine," Submitt. to Energies, 2015.

[21] R. Beckers, "Small Wind Turbine Site Selection," 2006, curled from https//www.solacity.com/small-wind-turbine-site-selection/.

[22] Spirn, Anne Whiston. "Air Quality At Street-Level: Strategies For Urban Design". Prepared for: Boston Redevelopment Authority, June1986

[23] Statistical data (between 1968-19770, Data Processing Division, Department of Meteorology, Thailand, 1999


★★★